JACS
JOURNAL OF THE AMERICAN CHEMICAL SOCIETY
Article
pubs.acs.org/JACS

Comparative Study of Microscopic Charge Dynamics in Crystalline Acceptor-Substituted Oligothiophenes

Manuel Schrader,[†] Roland Fitzner,[‡] Moritz Hein,[§] Chris Elschner,[§] Björn Baumeier,[†] Karl Leo,[§] Moritz Riede,[§] Peter Bäuerle,[‡] and Denis Andrienko*,[†]

[†]Max Planck Institute for Polymer Research, Ackermannweg 10, 55128 Mainz, Germany

[‡]Institute of Organic Chemistry II and Advanced Materials, Albert-Einstein-Allee 11, 89081 Ulm, Germany

[§]Institut für Angewandte Photophysik, Technische Universität Dresden, George-Bähr-Strasse 1, 01069 Dresden, Germany

Supporting Information

ABSTRACT: By performing microscopic charge transport simulations for a set of crystalline dicyanovinyl-substituted oligothiophenes, we find that the internal acceptor−donor−acceptor molecular architecture combined with thermal fluctuations of dihedral angles results in large variations of local electric fields, substantial energetic disorder, and pronounced Poole−Frenkel behavior, which is unexpected for crystalline compounds. We show that the presence of static molecular dipoles causes large energetic disorder, which is mostly reduced not by compensation of dipole moments in a unit cell but by molecular polarizabilities. In addition, the presence of a well-defined π-stacking direction with strong electronic couplings and short intermolecular distances turns out to be disadvantageous for efficient charge transport since it inhibits other transport directions and is prone to charge trapping.

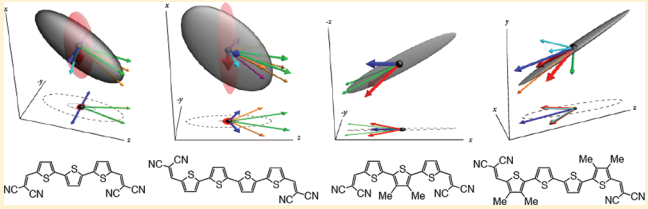

1. INTRODUCTION

The fabrication of flexible solar cells is one of the potential applications of organic semiconductors.[1−3] In spite of recent advancements to improve power conversion,[4−6] efficiency still remains a major factor which limits cost-effective mass production of organic solar cells.

Small dielectric screening and the corresponding large exciton binding energies of the photoactive layer require donor−acceptor interfaces to assist exciton splitting into free charges. Due to appropriate level alignment and electron transporting properties, fullerenes and its derivatives are widely used as acceptors, while the chemical structure of the donor is tuned to maximize the cell efficiency.[7] In particular, significant efforts are put into engineering molecules that have a lower optical gap, since the highest solar flux is found for green light with a photon energy around 2.0−2.5 eV.[4,8] Often this is achieved by attaching electron-withdrawing groups to a conjugated backbone, resulting in an internal donor−acceptor molecular architecture.[9−18] A typical example is terminally dicyanovinyl-substituted oligothiophenes (DCV*n*T), where this is realized by covalently binding strong electron-withdrawing dicyanovinyl (DCV) groups to an electron-donating oligothiophene core. Thin films of these compounds as well as blends with fullerene can be processed to have crystalline properties,[9,19] which is argued to be beneficial for charge transport. These are also of practical interest, since bulk heterojunction solar cells with DCV5T as a donor showed efficiencies of 5.2%.[19]

In this work we analyze charge transport in four crystalline dicyanovinyl-substituted oligothiophene derivatives, whose molecular structures are shown in Figure 1. These, chemically similar, compounds have all been crystallized by thermal gradient sublimation and characterized experimentally by X-ray structure analysis,[1,19] making it possible to systematically relate macroscopic mobility to microscopic charge-transfer quantities and underlying molecular structures.

To this end, hole transport is modeled by performing atomistic molecular dynamics simulations of crystal supercells, evaluating charge-hopping rates between neighboring molecules, and solving the master equation for a charge drift-diffusing in a box with periodic boundary conditions in an applied electric field using the kinetic Monte Carlo (KMC) algorithm.[20−26] The high-temperature limit of Marcus theory[27,28] is employed to evaluate charge-hopping rates between molecules:

$$\omega = \frac{J^2}{\hbar}\sqrt{\frac{\pi}{\lambda k_B T}}\exp\left[-\frac{(\Delta E-\lambda)^2}{4\lambda k_B T}\right] \quad (1)$$

where T is the temperature, λ is the reorganization energy, J is the electronic coupling element or transfer integral, and ΔE is the site energy difference which has contributions from an external electric field and electrostatic interactions, including polarization. These microscopic quantities are calculated

Received: January 26, 2012
Published: March 15, 2012

dx.doi.org/10.1021/ja300851q | *J. Am. Chem. Soc.* 2012, 134, 6052−6056

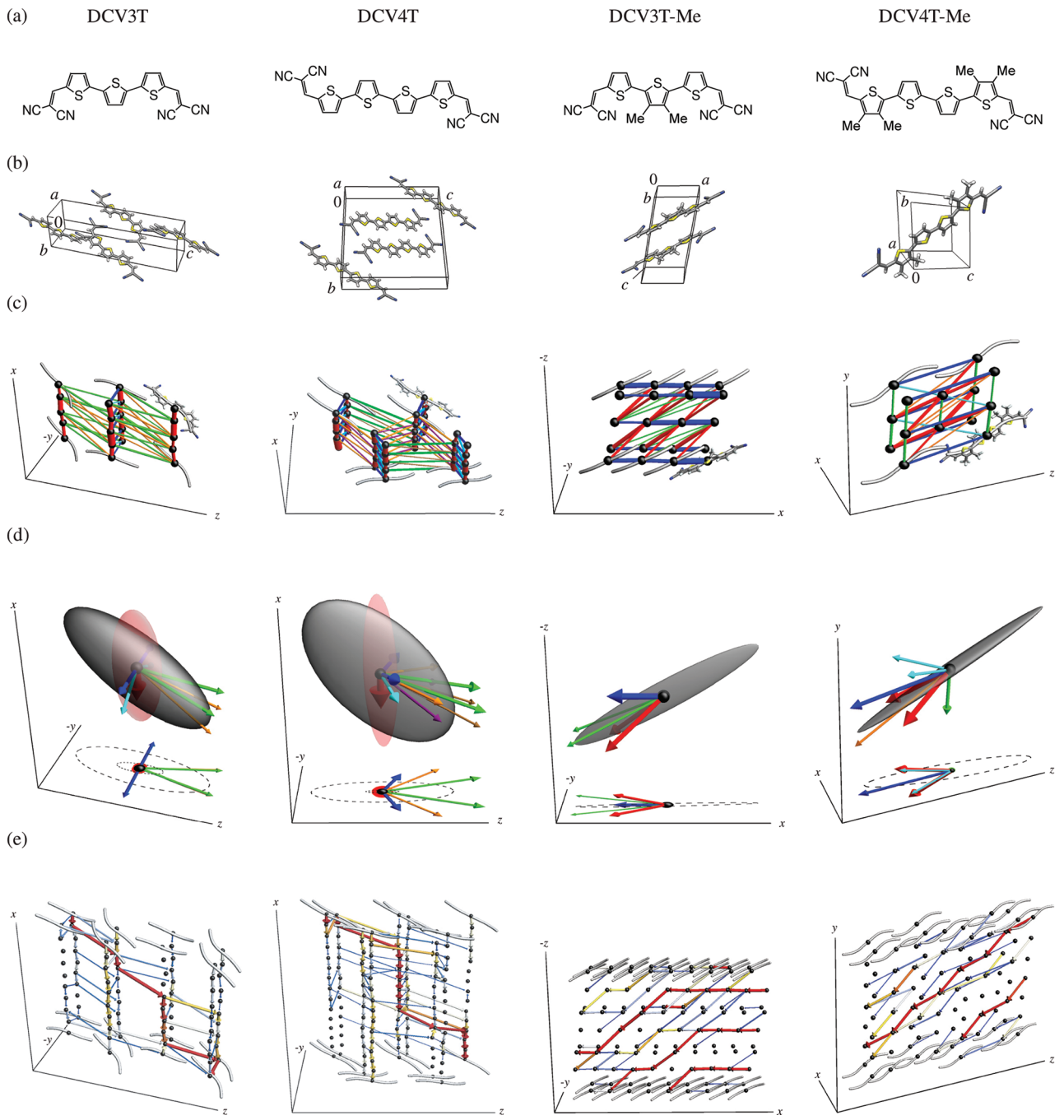

Figure 1. (a) Molecular structures of the compounds studied in this work. (b) Unit cells (see the Supporting Information). (c) Connectivity graphs based on the strength (line thickness) and direction (line color) of electronic couplings. The corresponding averages and distributions are provided in the Supporting Information. (d) Zero-field mobility tensor without (red) and with (gray) energetic disorder. The eigenvectors and the square root of the eigenvalues of $\hat{\boldsymbol{\mu}}$ (provided in the Supporting Information) define the principle axes and the equatorial radii of this ellipsoid. Arrows indicate the directions of the charge percolating network. For methylated compounds, red and gray ellipsoids have similar orientations, and hence only gray ellipsoids are shown. (e) Edge currents under an electric field of 800 $(V/cm)^{1/2}$ applied in the main transport direction (given by mobility tensor eigenvector with the highest eigenvalue or the longest axis of the gray ellipsoid in panel (d)). Arrows indicate the direction of the current, while the thickness and the color of the lines are proportional to the logarithm of the current amplitude. For clarity, different perspectives of (c) are shown in the Supporting Information.

explicitly for each pair of molecules in the crystal from quantum chemical calculations, as described below.

2. RESULTS

First-principles calculations are performed using the GAUSSIAN[29] package, molecular dynamics simulations using the GROMACS[30] package, polarized site energy calculations (Thole model)[31] using the TINKER package,[32] and charge transport simulations using the VOTCA[26,33] package. Technical details can be found in the Supporting Information.

2.1. Molecular Conformations. Analysis of molecular conformations in supercells consisting of 2880 molecules at 300 K shows that molecules are on average flat, in agreement with the experimental crystal structures (see the Supporting

dx.doi.org/10.1021/ja300851q | J. Am. Chem. Soc. 2012, 134, 6052−6056

Information). This is expected for nonalkylated oligomers DCV3T and DCV4T which have planar geometries of vacuum-optimized molecules. DCV3T-Me_2 and DCV4T-Me_4 are however twisted in their calculated ground-state geometries, and their planarization in the crystal is due to nonbonded interactions with neighboring molecules. As we will see, this has an important consequence for reorganization energies.

In every snapshot, molecules can significantly deviate from their average conformations due to thermal fluctuations. To quantify these deviations, the ensemble distributions of all dihedral angles in one molecular dynamics snapshot are shown in the Supporting Information. Their width is of the order of 20° for the thiophene−thiophene and 30° for the DCV−thiophene dihedral angles. This conformational disorder leads to site energy disorder, as will be shown below.

2.2. Reorganization Energy. The reorganization energy, λ, is one of the ingredients entering the charge-transfer rate, eq 1. It takes into account the change in nuclear degrees of freedom as the charge moves between two molecules. Optimizing the geometries of neutral and charged DCV*n*Ts with the dihedral angles constrained to their averages in the crystal, we obtain similar values of λ for all four compounds, as given in Table 1. When the calculation is based on unconstrained geometry optimizations, as is usually done, the resulting reorganization energies of alkylated DCV3T-Me_2 and DCV4T-Me_4 are larger by 0.15 and 0.13 eV, respectively. This is due to their twisted neutral ground-state geometry (all cations are flat) and the additional energy dissipated when charging a methylated molecule. Note that the lower values of λ lead to an order of magnitude increase of calculated mobilities.

Table 1. Density (ρ), Reorganization Energy (λ), Energetic Disorder (σ), and the Largest Eigenvalue of the Mobility Tensor (μ)

	DCV3T	DCV4T	DCV3T-Me_2	DCV4T-Me_4
ρ (g/cm^3)	1.25	1.23	1.37	1.45
λ (eV)	0.21	0.19	0.16	0.19
σ (eV)	0.11	0.10	0.08	0.07
μ (cm^2/(V s))	1.6×10^{-3}	1.1×10^{-3}	1.7×10^{-1}	1.6×10^{-1}

2.3. Electronic Coupling Elements. Electronic couplings, J^2, between neighboring molecules are often used to identify directionality and dimensionality of the charge percolating network. To analyze the topological connectivity of this network, the electronic coupling elements are visualized in Figure 1c.

One can see that DCV3T and DCV4T have a well-defined π-stacking direction (red), with the average coupling of 10^{-3} eV^2. The other directions (blue and green, perpendicular to the π-stacking) have several orders of magnitude lower couplings (see the Supporting Information). In contrast, the methylated compounds do not have a pronounced π-stacking with such strong couplings, instead the percolating network is composed of several directions of moderate couplings.

2.4. Site Energies. An important consequence of the conformational disorder is that it leads to fluctuations of electrostatic multipoles, e.g., molecular dipole moments. In amorphous systems, randomly oriented dipoles are known to lead to spatially correlated energetic disorder.[26,34−36] The widths of site energy distributions, σ, summarized in Table 1, show that the studied crystalline compounds also have substantial energetic disorder. In our case the conformational disorder is responsible for this disorder.

Note that DCV3T and DCV3T-Me_2 have a nonzero dipole moment already in their equilibrium conformations. Even though this permanent dipole moment is compensated in a unit cell, its fluctuations induce local electric fields interacting with the charge carrier. If one takes into account unscreened Coulomb interactions only, the width of the site energy distribution is 0.17 eV for nonalkylated and 0.30 eV for methylated DCV3T. If polarization effects are additionally taken into account, the disorder is reduced to 0.11 and 0.08 eV, respectively. Hence, not only the compensation of dipole moments in a unit cell[37] but also large polarizabilities of molecules are important to reduce the energetic disorder.

DCV4T and DCV4T-Me_4 have zero dipole moments in their equilibrium conformations, and here fluctuations result in slightly smaller (but still substantial) energetic disorder than in DCV3T and DCV3T-Me_2.

2.5. Charge Mobility. In crystalline phases charge transport is often anisotropic. To determine the main transport directions and to link them to packing motives, we first study charge diffusion without an applied field. To separate the contributions of electronic couplings and site energy disorder, we initially consider a model system, without energetic disorder (site energies are set to zero) and then include the effect of site energies. In both cases the calculated mobility tensor, $\hat{\mu}$, is

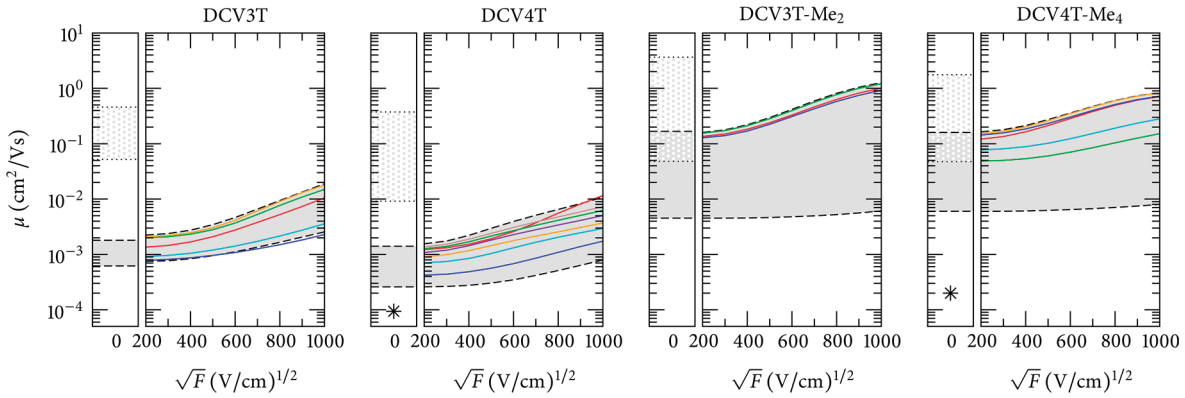

Figure 2. Hole mobilities as a function of an electric field applied along the largest and smallest principal axis directions of the diffusion tensor (dashed lines) and the other crystal directions (solid lines). Left panels indicate the range of zero-field mobilities with (filled) and without (dotted) energetic disorder. The measured OFET mobility for DCV4T and DCV4T-Me_4 is shown by dots.[1]

dx.doi.org/10.1021/ja300851q | J. Am. Chem. Soc. 2012, 134, 6052−6056

depicted as an ellipsoid in Figure 1d. The highest and lowest mobilities (which define the mobility range) are shown in the left panels of Figure 2.

In the absence of energetic disorder (red ellipsoids in Figure 1d), charge mobility of DCV3T and DCV4T is the highest along the π-stacking direction, which also has the strongest coupling. In methylated compounds, the π-stacking is not well-defined, and the direction of the highest mobility is a superposition of several transport directions with moderate couplings.

In spite of smaller (on average) coupling elements, methylated compounds have an order of magnitude higher mobilities, which can only be attributed to a better charge percolating network. This is a rather counterintuitive result: A pronounced π-stacking with strong electronic couplings in DCV3T and DCV4T is of disadvantage to an efficient charge transport. Microscopically, the one-dimensional π-stacking in bare compounds inhibits electronic couplings in other directions (see Figure 1c). Thus, methylated compounds have lower couplings but a better interconnected percolating network. Second, hopping sites in methylated compounds are positioned further apart from each other. In most cases, larger site−site separations generally lead to smaller mobilities, since electronic couplings (and hence the rates) decay exponentially with the separation, and local mobility is proportional to the rate times the separation. Molecules with extended π-conjugated systems, however, can have relative lateral shifts which do not change much the coupling (which is roughly proportional to the area of the overlap) but increase the center-of-mass (site−site) separation. In this case larger site−site separations result in longer charge hops and higher mobilities.

Switching on the energetic disorder (gray ellipsoids in Figure 1d) leads to an expected mobility reduction for all compounds. However, the mobility of DCV3T and DCV4T is reduced by 2 orders of magnitude, while for methylated compounds it is only a factor of 10. This difference cannot be completely attributed to a slightly smaller site energy disorder of methylated compounds (see Table 1 and the Supporting Information for the direction-resolved energetic disorder) but is mostly due to the aforementioned differences in percolating networks. Indeed, Figure 1d shows that the main transport directions of DCV3T and DCV4T are no longer aligned with the π-stacks. Such a reorientation of the mobility tensor is due to energetic defects (traps) in an one-dimensional π-stack. To avoid these traps, a charge carrier has to use one of the side directions with a weak coupling, as illustrated in Figure 1e. Here, edge currents show that a charge follows the π-stacking direction (red) until it reaches a trap and then hops to a neighboring π-stack. In the methylated compounds, the pathways consist of hops along several crystal directions of moderate couplings, and the charge can easily bypass traps and defects. Hence, large energetic disorder combined with a strong π-stacking is not beneficial for efficient transport.

One can conclude that methylation prevents molecules from strong π-stacking, leads to a favorable topology of charge percolating network with slightly lower couplings but larger site−site separations, and better interconnection of sites.

Another implication of the energetic disorder is a nonlinear dependence of mobility on the applied electric field or the Poole−Frenkel behavior. In our case the onset of this dependence can be seen already at moderate fields (ca. 400 $(V/cm)^{1/2}$, Figure 2), which indicates that the disorder is correlated (see the Supporting Information).

Experimental organic field-effect transistor (OFET) mobilities[1] for DCV4T and DCV4T-Me_4 are shown as dots in the left panels of Figure 2. Qualitatively, the experiments support simulation results in yielding a higher hole mobility for the methylated compound. A direct quantitative comparison cannot be made for two reasons: On one hand, the measurements have been performed on polycrystalline samples rather than on single crystals. Defects and grain boundaries impair charge transport, which might be the reason for systematically lower measured mobilities as compared to the simulated ones. On the other hand, OFETs operate at high charge carrier concentrations, while simulations are performed for a single carrier. Due to trap filling, charge mobility becomes less sensitive to energetic disorder at higher carrier concentrations.[38] This is a possible explanation for the smaller difference between DCV4T and DCV4T-Me_4 mobilities measured in OFETs as compared to the simulation result. Note that in solar cells, the charge carrier concentration is significantly lower than in OFETs and corresponds more closely to the simulated situation. Solar cells based on the alkylated DCV4T-Me_4 have shown higher efficiencies than those based on DCV4T,[1] indirectly supporting our conclusions of a better charge percolating network in DCV4T-Me_4.

3. CONCLUSIONS

To summarize, we have characterized structural and energetic disorder, performed simulations of hole transport, calculated zero-field mobility tensors and mobility field dependence, and visualized current pathways in supercells of four dicyanovinyl-oligothiophene derivatives.

The first observation is that the planarization of molecules in a crystal leads to a significant reduction of reorganization energies of methylated compounds (which are nonplanar in their neutral vacuum-optimized geometries) and hence to larger rates and higher charge mobilities.

Unexpectedly for crystalline compounds, we find that all systems have significant energetic disorder, which is attributed to charge distribution due to the donor−acceptor architecture and thermal fluctuations of dihedral angles. Moreover, in spite of the differences in static dipole moments, all compounds have similar site energy distributions. We show that this is a consequence of the large molecular polarizabilities and not due to the compensation of dipole moments in a unit cell.

Finally, it is often argued that good π-stacking with short intermolecular distances between molecules in a stack is beneficial for charge transport. We show that, for all studied compounds, the direction with the highest mobility is not parallel to the direction with the strongest coupling but is a superposition of several hopping directions. Moreover, for DCV3T and DCV4T, a pronounced π-stacking inhibits other transport directions. As a consequence, a charge cannot easily surpass traps created by the energetic disorder.

■ ASSOCIATED CONTENT

Supporting Information

Details of molecular dynamics simulations, force field parameters, and charge transport simulations are given. This material is available free of charge via the Internet at http://pubs.acs.org.

AUTHOR INFORMATION

Corresponding Author

denis.andrienko@mpip-mainz.mpg.de

Notes

The authors declare no competing financial interest.

ACKNOWLEDGMENTS

This work was partially supported by the DFG program IRTG 1404, DFG grant SPP 1355 and BMBF grant MESOMERIE. We are grateful to Mara Jochum and Carl Pölking for critical reading of the manuscript.

REFERENCES

(1) Fitzner, R.; Elschner, C.; Weil, M.; Uhrich, C.; Körner, C.; Riede, M.; Leo, K.; Pfeiffer, M.; Reinold, E.; Mena-Osteritz, E.; Bäuerle, P. *Adv. Mater.* **2012**, *24*, 675−680.

(2) Brédas, J.; Norton, J. E.; Cornil, J.; Coropceanu, V. *Acc. Chem. Res.* **2009**, *42* (11), 1691−1699.

(3) Kippelen, B.; Brédas, J. *Energy Environ. Sci.* **2009**, *2* (3), 251.

(4) Riede, M.; Mueller, T.; Tress, W.; Schueppel, R.; Leo, K. *Nanotechnology* **2008**, *19* (42), 424001.

(5) Brabec, C. J.; Gowrisanker, S.; Halls, J. J. M.; Laird, D.; Jia, S.; Williams, S. P. *Adv. Mater.* **2010**, *22* (34), 3839−3856.

(6) Grätzel, M. *Acc. Chem. Res.* **2009**, *42* (11), 1788−1798.

(7) Roncali, J. *Acc. Chem. Res.* **2009**, *42* (11), 1719−1730.

(8) Baumeier, B.; Andrienko, D.; Ma, Y.; Rohlfing, M. *J.Chem. Theory Comput.* **2012**, *8*, 997−1002.

(9) Ziehlke, H.; Fitzner, R.; Körner, C.; Gresser, R.; Reinold, E.; Bäuerle, P.; Leo, K.; Riede, M. K. *J. Phys. Chem. A* **2011**, *115* (30), 8437−8446.

(10) Wynands, D.; Mannig, B.; Riede, M.; Leo, K.; Brier, E.; Reinold, E.; Bäuerle, P. *J. Appl. Phys.* **2009**, *106* (5), 054509−054509−5.

(11) Schulze, K.; Uhrich, C.; Schüppel, R.; Leo, K.; Pfeiffer, M.; Brier, E.; Reinold, E.; Bäuerle, P. *Adv. Mater.* **2006**, *18* (21), 2872−2875.

(12) Yassar, A.; Videlot, C.; Jaafari, A. *Sol. Energy Mater. Sol. Cells* **2005**, *90*, 916−922.

(13) Xia, P. F.; Feng, X. J.; Lu, J.; Movileanu, R.; Tao, Y.; Baribeau, J.; Wong, M. S. *J. Phys. Chem. C* **2008**, *112* (42), 16714−16720.

(14) Xia, P. F.; Feng, X. J.; Lu, J.; Tsang, S.; Movileanu, R.; Tao, Y.; Wong, M. S. *Adv. Mater.* **2008**, *20* (24), 4810−4815.

(15) Li, Y.; Guo, Q.; Li, Z.; Pei, J.; Tian, W. *Energy Environ. Sci.* **2010**, *3* (10), 1427.

(16) Zhang, J.; Deng, D.; He, C.; He, Y.; Zhang, M.; Zhang, Z.; Zhang, Z.; Li, Y. *Chem. Mater.* **2011**, *23* (3), 817−822.

(17) Roquet, S.; Cravino, A.; Leriche, P.; Alévêque, O.; Frère, P.; Roncali, J. *J. Am. Chem. Soc.* **2006**, *128* (10), 3459−3466.

(18) Morana, M.; Azimi, H.; Dennler, G.; Egelhaaf, H.; Scharber, M.; Forberich, K.; Hauch, J.; Gaudiana, R.; Waller, D.; Zhu, Z.; Hingerl, K.; van Bavel, S. S.; Loos, J.; Brabec, C. J. *Adv. Funct. Mater.* **2010**, *20* (7), 1180−1188.

(19) Fitzner, R.; Reinold, E.; Mishra, A.; Mena-Osteritz, E.; Ziehlke, H.; Körner, C.; Leo, K.; Riede, M.; Weil, M.; Tsaryova, O.; Weiß, A.; Uhrich, C.; Pfeiffer, M.; Bäuerle, P. *Adv. Funct. Mater.* **2011**, *21* (5), 897−910.

(20) Vehoff, T.; Chung, Y. S.; Johnston, K.; Troisi, A.; Yoon, D. Y.; Andrienko, D. *J. Phys. Chem. C* **2010**, *114* (23), 10592−10597.

(21) Vehoff, T.; Baumeier, B.; Andrienko, D. *J. Chem. Phys.* **2010**, *133* (13), 134901−134901−4.

(22) Vehoff, T.; Baumeier, B.; Troisi, A.; Andrienko, D. *J. Am. Chem. Soc.* **2010**, *132* (33), 11702−11708.

(23) Rühle, V.; Kirkpatrick, J.; Andrienko, D. *J. Chem. Phys.* **2010**, *132* (13), 134103−134103−9.

(24) Lukyanov, A.; Andrienko, D. *Phys. Rev. B* **2010**, *82* (19), 193202.

(25) May, F.; Marcon, V.; Hansen, M. R.; Grozema, F.; Andrienko, D. *J. Mater. Chem.* **2011**, *21* (26), 9538−9545.

(26) Rühle, V.; Lukyanov, A.; May, F.; Schrader, M.; Vehoff, T.; Kirkpatrick, J.; Baumeier, B.; Andrienko, D. *J. Chem. Theory Comput.* **2011**, *7* (10), 3335−3345.

(27) Marcus, R. A. *Rev. Mod. Phys.* **1993**, *65* (3), 599.

(28) Hutchison, G. R.; Ratner, M. A.; Marks, T. J. *J. Am. Chem. Soc.* **2005**, *127* (7), 2339−2350.

(29) Frisch, M. J.; Jaramillo, J.; Gomperts, R.; Stratmann, R. E.; Yazyev, O.; Austin, A. J.; Cammi, R.; Pomelli, C.; Ochterski, J. W.; Ayala, P. Y.; Morokuma, K.; Voth, G. A.; Salvador, P.; Dannenberg, J. J.; Zakrzewski, V. G.; Dapprich, S.; Daniels, A. D.; Strain, M. C.; Farkas, O.; Malick, D. K.; Rabuck, A. D.; Raghavachari, K.; Foresman, J. B.; Ortiz, J. V.; Cui, Q.; Baboul, A. G.; Clifford, S.; Cioslowski, J.; Stefanov, B. B.; Liu, G.; Liashenko, A.; Piskorz, P.; Komaromi, I.; Martin, R. L.; Fox, D. J.; Keith, T.; Al-Laham, M. A.; Peng, C. Y.; Nanayakkara, A.; Challacombe, M.; Gill, P. M. W.; Johnson, B.; Chen, W.; Wong, M. W.; Gonzalez, C.; Pople, J. A. *Gaussian 03*, revision C.02; Gaussian, Inc.: Wallingford, CT, 2004.

(30) Hess, B.; Kutzner, C.; van der Spoel, D.; Lindahl, E. *J. Chem. Theory Comput.* **2008**, *4* (3), 435−447.

(31) Thole, B. *Chem. Phys.* **1981**, *59* (3), 341−350.

(32) Ponder, J. W.; Wu, C.; Ren, P.; Pande, V. S.; Chodera, J. D.; Schnieders, M. J.; Haque, I.; Mobley, D. L.; Lambrecht, D. S.; DiStasio, R. A.; Head-Gordon, M.; Clark, G. N. I.; Johnson, M. E.; Head-Gordon, T. *J. Phys. Chem. B* **2010**, *114* (8), 2549−2564.

(33) Rühle, V.; Junghans, C.; Lukyanov, A.; Kremer, K.; Andrienko, D. *J. Chem. Theory. Comput.* **2009**, *5* (12), 3211−3223.

(34) Novikov, S. V.; Vannikov, A. V. *J. Phys. Chem.* **1995**, *99* (40), 14573−14576.

(35) Novikov, S. V.; Dunlap, D. H.; Kenkre, V. M.; Parris, P. E.; Vannikov, A. V. *Phys. Rev. Lett.* **1998**, *81* (20), 4472.

(36) Nagata, Y.; Lennartz, C. *J. Chem. Phys.* **2008**, *129* (3), 034709.

(37) Würthner, F.; Kaiser, T. E.; Saha-Möller, C. R. *Angew. Chem., Int. Ed.* **2011**, *50* (15), 3376−3410.

(38) Pasveer, W.; Cottaar, J.; Tanase, C.; Coehoorn, R.; Bobbert, P.; Blom, P.; de Leeuw, D.; Michels, M. *Phys. Rev. Lett.*, **2005**, *94*(20), 206601.